Nanoscale phase separation in deeply underdoped Bi_{2}Sr_{2}CuO_{6+δ} and Ca_{2}CuO_{2}Cl_{2}

Peter Mistark, Robert S. Markiewicz, and Arun Bansil

Phys. Rev. B **91**, 140501 — Published 6 April 2015

DOI: 10.1103/PhysRevB.91.140501

Nanoscale phase separation in deep underdoped $Bi_2Sr_2CuO_{6+\delta}$ and $Ca_2CuO_2Cl_2$

Peter Mistark, Robert S. Markiewicz, Arun Bansil
Department of Physics, Northeastern University, Boston, Massachusetts 02115, USA
(Dated: Version of March 19, 2015)

We demonstrate that the tunneling spectra from deeply underdoped $Bi_2Sr_2CuO_{6+\delta}$ (Bi2201) and $Ca_2CuO_2Cl_2$ (CCOC) provide clear evidence for a nanoscale phase separation (NPS), which causes the gap to fill rather than close with doping. The phase separation extends from half-filling to a doping of $x \sim 0.09$. Assuming that the NPS is in the form of stripes, the nodal gap, which we model as a Coulomb gap, arises from impurity pinning of the charged stripes, and ultimately drives a metal-insulator transition.

PACS numbers: 74.72.Gh, 74.72.Cj, 74.25.Dw, 74.25.Jb

Just how a correlated material evolves from being a Mott insulator into a high-T_c superconductor remains a highly contentious issue nearly three decades after the discovery of the cuprates with important implications for the underlying mechanism of superconductivity. A major puzzle concerns what happens to the 2 eV gap present in the half-filled Mott insulator when it is doped. Various theoretical models make clear predictions in this connection. In strong coupling theories ($t-J$ or the $U \to \infty$ Hubbard model) the gap remains large, but there is an anomalous spectral weight transfer (ASWT) from the upper (UMB) to the lower magnetic band (LMB)[1]. The width of the LMB gradually increases from $\sim 2J$ to $\sim 8t$ as doping changes from $x=0$ to $x=1$. For the smaller-U Hubbard models, the ASWT is actually faster, as electrons can lower their kinetic energy by hopping through occupied states. In the intermediate coupling models[2], this is associated with a decrease of the magnetic gap with doping.[3]

In order to explain the rapid changes observed at low doping, one would require doping-dependent screening of the effective Hubbard U: In a two-dimensional system with a magnetic gap, the screening would, in fact, need to turn on discontinuously with doping away from half-filling[4]. In such a case, Mott showed that the transition would be first order.[5] This would present a very different scenario for the doping dependence of the gap, leading to a filling in rather than a closing of the gap as islands of doped phase appear in the sample. Here we compare and contrast the various scenarios in the light of recent scanning tunneling microscopy/spectroscopy (STM/STS) experiments on the cuprates.

Experimental data in the deeply underdoped regime, which could help discriminate between different theoretical scenarios, have been difficult to obtain until recently. Photoemission is unable to probe the Mott gap as it only sees the filled states. STM finds only a ~ 100 meV pseudogap[6] without revealing how this gap is connected to the 2 eV optical gap at half-filling. Resonant inelastic x-ray scattering (RIXS) provides evidence of gap collapse, but since it measures a joint density of states (DOS), the analysis is model dependent[7]. Very recent STM data from CCOC[8] and Bi2201[9] give new insight into this problem as these data show the presence of a large gap at half-filling, comparable to the optical gap. Remarkably, the gap in the STM spectra neither remains unchanged nor shrinks with doping, but instead it fills in. This observed behavior is not consistent with a uniform doping scenario. A possible explanation is provided by a model involving competing magnetic orders in which there can be a phase separation between the undoped insulator and an incommensurate magnetic phase near 1/8 doping[10]. Since the positive ions are fixed in the lattice, this electronic phase separation cannot be macroscopic, but must be a NPS, possibly in the form of stripes.

Here we show how the recent STS data on deeply underdoped cuprates can be understood within the framework of an intermediate coupling model.[11] The band dispersion is taken from density functional theory (DFT) calculations, renormalized to account for the effects of electronic correlations[3, 12], while the magnetic order is calculated self-consistently within the random phase approximation (RPA). We use a mean field treatment of the Hubbard model given by the Hamiltonian

$$\begin{aligned} H = &\sum_{\mathbf{k},\sigma} (\epsilon_{\mathbf{k}} - \epsilon_F) c^\dagger_{\mathbf{k},\sigma} c_{\mathbf{k},\sigma} \\ &+ \Delta_{AF} \sum_{\mathbf{k},\mathbf{k'}} [c^\dagger_{\mathbf{k}+\mathbf{Q},\uparrow} c_{\mathbf{k},\uparrow} - c^\dagger_{\mathbf{k'}-\mathbf{Q},\downarrow} c_{\mathbf{k'},\downarrow}] \\ &+ \sum_{\mathbf{k}} [\Delta_{\mathbf{k}} c^\dagger_{\mathbf{k},\uparrow} c^\dagger_{-\mathbf{k},\downarrow} + \Delta^*_{\mathbf{k}} c_{-\mathbf{k},\downarrow} c_{\mathbf{k},\uparrow}], \end{aligned} \tag{1}$$

where $c^\dagger_{\mathbf{k},\sigma}$ ($c_{\mathbf{k},\sigma}$) are the creation (annihilation) operators for an electron at momentum $\mathbf{k}$ with spin σ, $\epsilon_{\mathbf{k}}$ is the corresponding non-interacting energy level, ϵ_F is the Fermi energy, and $\mathbf{Q} = (\pi, \pi)$. Δ_{AF} is the antiferromagnetic (AF) order parameter, and $\Delta_{\mathbf{k}}$ is the d-wave superconducting (SC) gap function with $\Delta_{\mathbf{k}} = \Delta_0(cos(k_x a) - cos(k_y a))/2$, where Δ_0 is the superconducting order parameter.

The band dispersion of the non-interacting system, $\epsilon_{\mathbf{k}}$,

is modeled in the tight binding form:

$$\begin{aligned}\epsilon_{\mathbf{k}} = & -2t[c_x(a)+c_y(a)] \\ & -4t'c_x(a)c_y(a) - 2t''[c_x(2a)+c_y(2a)] \\ & -4t'''[c_x(2a)c_y(a)+c_y(2a)c_x(a)] \\ & -4t^{iv}c_x(2a)c_y(2a), \end{aligned} \quad (2)$$

in terms of the tight binding parameters t^i. Here, $c_i(\alpha a) = cos(\alpha \mathbf{k}_i a)$, and a is the lattice constant. The tight binding parameters for CCOC determined through a fit to the corresponding DFT calculations[13, 14] are: $t = 0.36$eV, $t' = -0.1$eV, $t'' = 0.035$eV, and $t''' = 0.01$eV. The tight binding parameters for Bi2201, which are taken from an experimental fit [15] are: $t = 0.22$eV, $t' = -0.034315$eV, $t'' = 0.035977$eV. $t''' = -0.0071637$eV.

The Δ_{AF} term in the Hamiltonian splits the quasiparticle spectrum into two bands, where $\nu = +$ and $\nu = -$ represent the UMB and LMB, respectively. These bands are again split by the SC order, resulting in a total of four bands with dispersions given by:

$$E^{\nu}_{\mathbf{k}} = \pm\sqrt{\left(E^{s,\nu}_{k}\right)^2 + \Delta^2_k}. \quad (3)$$

where $\xi_{\mathbf{k}} = \epsilon_{\mathbf{k}} - \epsilon_F$ and $\xi^{\pm}_{\mathbf{k}} = (\xi_{\mathbf{k}} \pm \xi_{\mathbf{k}+\mathbf{Q}})/2$. $E^{s,\nu}_{\mathbf{k}} = \xi^{+}_{\mathbf{k}} + \nu E_{0k}$, with $E_{0\mathbf{k}} = \sqrt{\left(\xi^{-}_{\mathbf{k}}\right)^2 + (US)^2}$ describes the quasiparticle dispersion in the absence of superconducting order. The transformation between the momentum and quasiparticle spaces involves the coherence factors

$$\begin{aligned}\alpha_{\mathbf{k}}(\beta_{\mathbf{k}}) &= \sqrt{(1 \pm \xi^{-}_{\mathbf{k}}/E_{0\mathbf{k}})/2}, \\ u^{\nu}_{\mathbf{k}}(v^{\nu}_{\mathbf{k}}) &= \sqrt{[1 \pm (\xi^{+}_{\mathbf{k}} + \nu E_{0\mathbf{k}})/E^{\nu}_{\mathbf{k}}]/2}. \end{aligned} \quad (4)$$

The self-consistent equations for the superconducting gap parameter Δ_0 and the staggered magnetization, S, where $\Delta_{AF} = SU$ are

$$\begin{aligned}\Delta_0 = & -V\sum_{\mathbf{k}} g_{\mathbf{k}} \\ & \times \left[u^{+}_{\mathbf{k}}v^{+}_{\mathbf{k}} \tanh\left(\beta E^{+}_{\mathbf{k}}/2\right) + u^{-}_{\mathbf{k}}v^{-}_{\mathbf{k}} \tanh\left(\beta E^{-}_{\mathbf{k}}/2\right)\right] \\ = & -V\Delta_0 \sum_{\mathbf{k}} g^2_{\mathbf{k}} \\ & \times \left[\frac{1}{2E^{+}_{\mathbf{k}}} \tanh\left(\beta E^{+}_{\mathbf{k}}/2\right) + \frac{1}{2E^{-}_{\mathbf{k}}} \tanh\left(\beta E^{-}_{\mathbf{k}}/2\right)\right], \end{aligned} \quad (5)$$

$$\begin{aligned} S = & \frac{1}{N}\sum_{\mathbf{k}} \alpha_{\mathbf{k}}\beta_{\mathbf{k}} \\ & \times\left[\left((v^{-}_{\mathbf{k}})^2 - (v^{+}_{\mathbf{k}})^2\right) + \left((v^{+}_{\mathbf{k}})^2 - (u^{+}_{\mathbf{k}})^2\right) f(E^{+}_{\mathbf{k}})\right. \\ & \left. -\left((v^{-}_{\mathbf{k}})^2 - (u^{-}_{\mathbf{k}})^2\right) f(E^{-}_{\mathbf{k}})\right], \\ = & \frac{US}{N}\sum_{\mathbf{k}} \frac{1}{4E_{0\mathbf{k}}} \\ & \times \left[\frac{E^{s,+}_{\mathbf{k}}}{E^{+}_{\mathbf{k}}} \tanh\left(\beta E^{+}_{\mathbf{k}}/2\right) - \frac{E^{s,-}_{\mathbf{k}}}{E^{-}_{\mathbf{k}}} \tanh\left(\beta E^{-}_{\mathbf{k}}/2\right)\right], \end{aligned} \quad (6)$$

where in equation 5, V is the superconducting potential and $g_{\mathbf{k}} = cos(k_x) - cos(k_y)$.

In the undoped CCOC, our model predicts a large, ~ 2 eV gap at half filling, consistent with experiment[8] as seen in Fig.2(c). We find that the AF gap parameter, $2\Delta_{AF} = 2.76eV$, is approximately equal to the energy difference between the top of the LMB and the VHS of the UMB. Moreover, the same model reproduces the experimental dispersions and density of states (DOS) for $x \geq 0.1$, in both Bi2201[16] and $Bi_2Sr_2CaCu_2O_{8+\delta}$ (Bi2212)[11].

For a uniformly doped system, the AF gap at half-filling would decrease steadily with doping, leaving only a small pseudogap, as illustrated for Bi2201 in Fig. 1. In contrast, recent STM experiments on deeply underdoped CCOC and Bi2201 reveal a more complicated doping evolution, where a strong growth of in-gap states in the local DOS is observed in the spectra.[8, 9] Our analysis will show that these results can be understood in terms of a NPS. While NPS can have different spatial patterns, including stripes, dots, or polarons, stripes seem to be favored in $La_{2-x}Sr_xCuO_4$ (LSCO)[17–19] and Bi2201[20] as they provide a natural explanation for the Yamada plot[21].

In the cuprates, there are several sources of charge inhomogeneity that may act in parallel. First, a charge-density wave phase has been reported in a number of cuprates[22–28]. Then, STM studies find patches of varying local density, which are mainly correlated with oxygen vacancies in the Bi-cuprates.[29] Finally, a phase separation has been predicted in Bi-cuprates, most notably between the insulating phase in the undoped compound and at a doping around $x = 0.125$,[10] which as already noted would lead to NPS. We emphasize that NPS differs from a macroscopic phase separation in that in the latter case only two densities are involved, so that properties such as the AF and SC gaps will be doping independent. In the NPS scenario, the individual domains are so small that properties will evolve with doping in each domain type due to the proximity of other domains.[30, 31] For instance, in oxygen-doped $La_2CuO_{4+\delta}$, the excess oxygen remains mobile down to below room temperature. This results in a macroscopic phase separation over a wide doping range where the SC transition temperature T_c has a fixed value close to that at optimal doping, while the AF Néel temperature remains nearly unchanged from its value at zero doping.[32] In contrast, in Sr-doped LSCO, the Sr ions are immobile, and a macroscopic phase separation is replaced by spin-and-charge stripes[17], which can be a form of NPS, while T_c varies smoothly with x.

The main effect of nanoscale proximity of domains is to produce relatively small shifts in the DOSs associated with the end phases: for example, the undoped insulator phase might acquire a small hole doping[31, 33]. Here we simplify the analysis by assuming that in a NPS model of stripes, the total DOS is approximately given by the

superposition of the DOSs of the two end phases.

The DOSs for the end phases of Bi2201 and CCOC used in this article have been obtained within the framework of the quasi-particle GW (QP-GW) scheme for modeling the electronic structures of the cuprates.[2] The only essential parameters involved in the QP-GW scheme are the material specific tight-binding band parameters and the value of the Hubbard U at half-filling. The doping dependent electronic structure is then determined via a self-consistently computed self-energy correction, which accounts for strong correlation effects within an intermediate coupling scenario. A key feature of the scheme is that the low energy uncorrelated DFT based states near the Fermi energy are renormalized and broadened due to charge and magnetic fluctuations in the presence of AF and SC orders, in addition to the appearance of high energy features in the electronic spectrum, which reflect remnants of Mott physics. Notably, the theory predicts the value of the low-energy dispersion renormalization factor, Z,in a doping dependent manner. The renormalization factor Z is determined self consistently within the QP-GW scheme. For details of these and other aspects of the QP-GW scheme we refer the reader to a recent review[2], which discusses the methodology and its extensive applications, and shows how this scheme reasonably captures many salient features of the doping and temperature dependent spectra of the cuprates.

Figure 2 displays the DOS calculated in the NPS model for Bi2201 and CCOC within the QP-GW scheme. The dopings for CCOC correspond to the STM data of Ref. 8, which is plotted along with the calculated curves in frames (c) and (d), assuming that each patch contains a stripe-like mix of two phases. For Bi2201, in Figs. 2(a,b), we invoke two stable phases one with x_0 = 0.0, U/t = 7.576, and Z = 0.9, and the other with x_1 = 0.09, U/t = 3.576, and Z = 0.7. Linear combinations of these DOSs are then generated to represent an average doping, x_{av}, where x_{av} = 0.03 in Fig. 2(a) and 0.08 in Fig. 2(b). For CCOC, Figs. 2(c,d), the stable phases have x_0 = 0.0 with U/t = 8.5, Z = 1 and x_1 = 0.09 with U/t = 3.3, Z = 0.5. In our model, x_0 corresponds to half-filling and gives the experimentally observed large gap, x_1 is taken to be the doping which reproduces the DOS of the in-gap states, and Z is determined self-consistently within the QP-GW scheme[2]. For Bi2201 we used the effective U/t calculated in Ref.[34], fit to a decaying exponential $U/t = a_1 e^{-x/b} + a_2$, where a_1 = 4.626, a_2 = 2.95, and b = 0.045. The resulting self-consistent values of Δ_{AF} are shown in Fig. 1(e). For CCOC, values of U are chosen such that the self-consistent Δ_{AF}'s give the DOSs that match the experimental large gap and in-gap states in ref. 8 for x_0 and x_1, respectively. This simple picture is seen in Fig. 2 to reproduce the effect of *gap-filling* as a function of doping, rather than the gap-closing shown in Fig. 1. In Figs. 2(c,d) the model calculations are in good accord with the corresponding experimental data

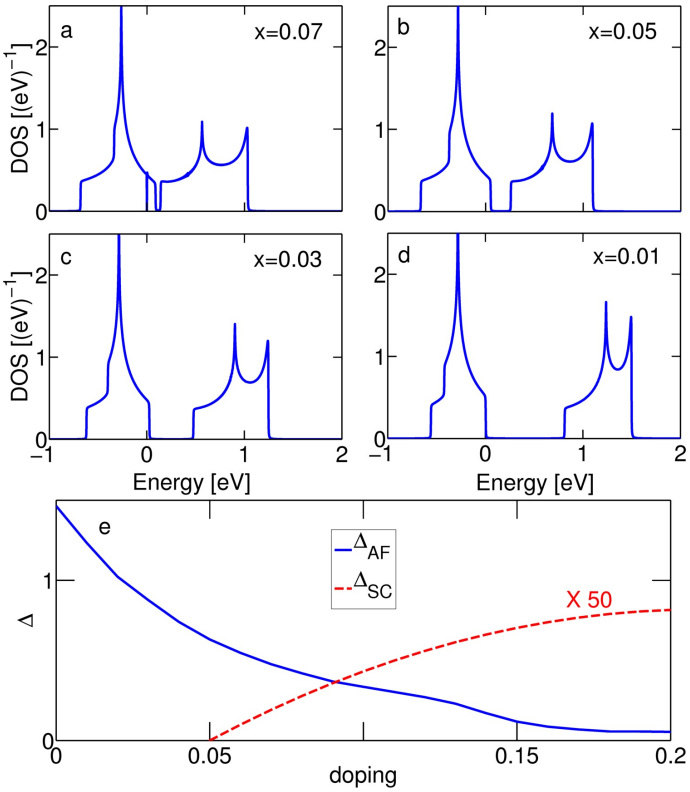

FIG. 1. (Color online) (a-d) DOS for uniformly doped Bi2201 with AF + SC orders at four different dopings x. Fermi energy is defined to be zero. The dip near zero energy in (a) is due to the SC gap. (e) Two gap scenario, showing self-consistent values of Δ_{AF} (solid blue line) and Δ_0 (dashed red line) vs doping. The Δ_0 curve is scaled up by 50 for clarity.

(solid lines with noise). The model captures both the gap edge and the DOS peak (subband Van Hove singularity), and, for the doped sample, the in-gap DOS. Note that at energies < -1 eV or > 3 eV there is additional DOS weight associated with bands not included in the present modeling.

Fig. 3 compares our model calculations with data from Ref. 6 over a narrow energy range. It is important to recognize here that at low energies the system undergoes a metal-insulator transition associated with a nodal gap[6, 35–38]. Within the present model, this gap arises on the charged stripes (regions of higher doping) and increases as the doping decreases and the stripes separate further. Assuming this to be an effect of stripe pinning by impurities, we model it as a Coulomb gap[39], as has been suggested previously[36, 40]. The Coulomb gap is a soft gap arising from the Coulomb interaction of particles on impurity sites, and its effect on the DOS (in a two-dimensional system) can be calculated self-consistently via the following equation[39]:

$$g(\omega) = \Delta exp\left(-\int_0^\infty \frac{g(\omega')d\omega'}{(\omega+\omega')^2}\right), \qquad (7)$$

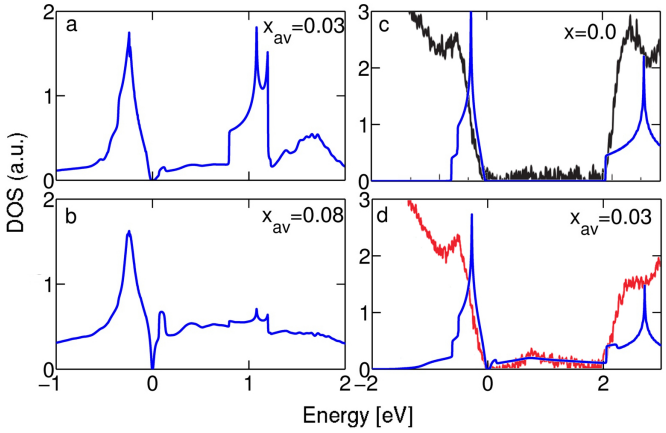

FIG. 2. (Color online) DOS for the AF system in the presence of a NPS for $x_{av} = 0.03$ (a) and 0.08 (b) for Bi2201[43]. (c) Calculated DOS at half-filling (solid blue line) for CCOC compared to the corresponding STM data[8] (black curve with noise). (d) Calculated DOS for the AF system with NPS in CCOC (solid blue line) compared to the corresponding experimental data[8] (solid red line with noise). STM intensities in (c,d) are scaled to match the Van Hove singularity below the Fermi energy[44].

where $g(\omega)$ is the DOS at frequency ω, and Δ is the width of the Coulomb gap. In our case, we multiply $g(\omega)$ by the DOS obtained from a QP-GW computation with AF order to simulate the presence of a Coulomb gap. Fig. 3 shows that the resulting DOS reproduces the characteristic features of the STM data quite well, including the peak above the Fermi energy due to the bottom of the UMB in the x_1 phase, the peak below the Fermi energy from the LMB in the x_0 phase, and the soft gap with zero states at the Fermi energy due to the Coulomb gap. Table I gives details of the parameters used for the model results (dashed curves) in Fig. 3 from top down. In order to minimize the number of parameters, we estimate the energy of the Coulomb gap from the experimental data. The onset temperature, T_0, of the Coulomb gap was derived from transport measurements given in Figure 4(c) of Ref. 36, and used to estimate the size of the gap assuming $2\Delta/k_BT_0 = 4$. Gap values for CCOC, determined in this way, are listed in Table I and Fig. 3.

The Coulomb gap is the natural result of pinning of stripe order by impurities. Therefore, it exists over the doping range, $0.00 \leq x_{av} \leq 0.09$, where we are modeling the NPS as a stripe order. As x_{av} moves away from half-filling, the magnitude of the Coulomb gap decreases to account for the shrinking width of magnetic stripes. If we ignore the Coulomb gap, spectral weight would be present at the Fermi energy as seen in the DOS of Fig. 1(b-d) resulting in a significant deviation from experimental results at low energies[6, 8]. Notably, the experimental data in Fig. 3 show that the soft gap closes at a point at the Fermi energy, whereas our computations yield a broad minimum which is symmetric around the Fermi energy. The simple model of DOS introduced in this study, however, is only meant to capture global features of an NPS with a Coulomb gap. A more sophisticated model should take into account the local topology of the NPS phase, and the details of the associated phase separation. For instance, in the low-doping regime, the doped-phase could take the form of islands or stripes, and these details will modify the nature of the resulting Coulomb gap. It may also be necessary to include disorder effects (see Fig. 65 of Ref. 18).

TABLE I. Value of Coulomb gap Δ and the corresponding average doping values, x_{av}, used in calculating the DOSs of CCOC shown in Fig. 3. The calculated curves from top to bottom in Fig. 3 correspond to DOS indices 1 through 9 in this table.

DOS index	$\Delta(meV)$	x_{av}
1	44.5	0.060
2	50.8	0.055
3	57.2	0.050
4	63.5	0.045
5	69.8	0.040
6	76.1	0.035
7	82.4	0.030
8	88.8	0.025
9	95.1	0.020

The role of NPS or 'stripe' physics near a Mott transition has been discussed often in the litertaure[17, 18, 41]. Note that NPS bears a resemblance to the strong-coupling effects, which give rise to ASWT with doping in the cuprates.[1] ASWT is generally interpreted in terms of Mott physics: there is a penalty U for putting a second electron on a copper site that is already occupied. When an electron is now removed from a given site, both holes lie at a low energy above the Fermi energy since there is no U-penalty for adding a hole with either spin. Thus, because of ASWT, the occupation of the upper Hubbard band is not fixed, but decreases with increased hole doping. In an intermediate coupling model, the Mott gap becomes an AF gap. In the presence of NPS, adding a hole creates a region of higher doping, where the AF gap is considerably smaller, so that the second hole is shifted to a much lower energy just as in ASWT (see Fig. 2). Finally, in the strong coupling regime, there is a tendency for atoms with two holes to cluster (to increase the kinetic energy without introducing a U-penalty), thus providing an additional link with NPS.

In conclusion, we have demonstrated that the gap-filling with doping, rather than gap-closing, observed experimentally in STM studies of deeply underdoped CCOC and Bi2201 is naturally understood in terms of a NPS[10]. Local stripes would be strongly pinned by

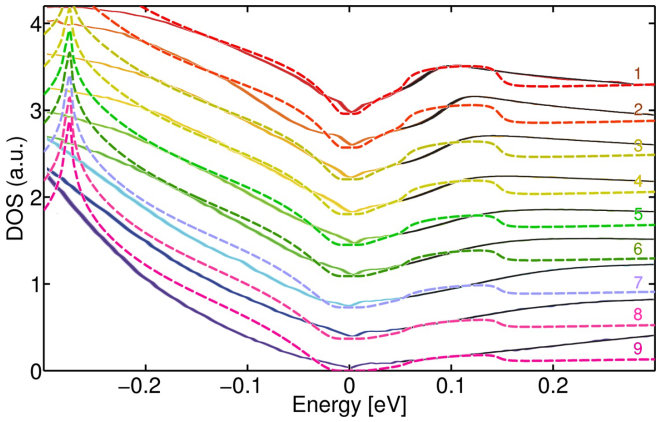

FIG. 3. (Color online) Calculated DOSs including Coulomb gap for modeling a NPS in an AF system (dashed lines) compared to the corresponding STM data from Ref. 6 (solid lines). The number next to a theoretical curve indicates the DOS index of that curve associated with Table I. The curves are shifted vertically for clarity. Different experimental curves correspond to DOS measured on different patches in a single CCOC sample.

impurities, explaining the occurrence of a nodal gap, a metal-insulator transition, and spin-glass-like phenomena found in underdoped cuprates. The NPS model also predicts[10] the coexistence of (π, π) AF order and an incommensurate SDW phase, as has been observed recently in LSCO[42].

Acknowledgments This research is supported by the US Department of Energy, Office of Science, Basic Energy Sciences contract DE-FG02-07ER46352, and benefited from Northeastern University's Advanced Scientific Computation Center (ASCC), and the allocation of supercomputer time at NERSC through grant number DE-AC02-05CH11231.

[1] H. Eskes, M.B.J. Meinders, and G.A. Sawatzky, Phys. Rev. Lett. **67**, 1035 (1991).
[2] T. Das, R. S. Markiewicz, and A. Bansil, Advances in Physics **63**, 151-266 (2014).
[3] R.S. Markiewicz, Tanmoy Das, and A. Bansil, Phys. Rev. B **82**, 224501 (2010).
[4] R.S. Markiewicz, Phys. Rev. B **70**, 174518 (2004).
[5] N.F. Mott, Phil. Mag B**50**, 161 (1984).
[6] Y. Kohsaka, T. Hanaguri, M. Azuma, M. Takano, J. C. Davis, H. Takagi. Nature Physics **8**, 534 (2012).
[7] R.S. Markiewicz and A. Bansil, Phys. Rev. Lett. **96**, 107005 (2006).
[8] Cun Ye, Peng Cai, Runze Yu, Xiaodong Zhou, Wei Ruan, Qingqing Liu, Changqing Jin, and Yayu Wang, Nature Communications **4**, 1365 (2013).
[9] Yayu Wang, SNS 2013.
[10] G. Seibold, R.S. Markiewicz, and J. Lorenzana, Phys. Rev. B **83**, 205108 (2011).
[11] J. Nieminen, I. Suominen, T. Das, R. S. Markiewicz, and A. Bansil. Phys. Rev. B. **85**, 214504 (2012).
[12] R.S. Markiewicz, S. Sahrakorpi, M. Lindroos, H. Lin, and A. Bansil, Phys. Rev. B **72**, 054519 (2005).
[13] Tight binding parameters for CCOC were approximated by the tight binding parameters for Bi2212 found in [11]. All tight-binding parameters are taken to be doping independent in the spirit of a rigid band model, which is expected to be a reasonable approximation for doping away from the cuprate planes. A more realistic treatment of the doping dependence of the electronic states using various approaches was not undertaken.[14]
[14] A. Bansil, R. S. Rao, P. E. Mijnarends and L. Schwartz, Phys. Rev. B23, 3608(1981); H. Lin, S. Sahrakorpi, R.S. Markiewicz, and A. Bansil, Phys. Rev. Lett. 96, 097001 (2006); L. Huisman, D. Nicholson, L. Schwartz and A. Bansil, Phys. Rev. B24, 1824(1981); S.N. Khanna, A.K. Ibrahim, S.W. McKnight, and A. Bansil, Solid State Commun. 55, 223 (1985).
[15] Rui-Hua He *et al.*, Science **331**, 1579 (2011).
[16] P. Mistark, H. Hasnain, R. S. Markiewicz, and A. Bansil. ArXiv:1403.2316.
[17] S.A. Kivelson, I.P. Bindloss, E. Fradkin, V. Oganesyan, J.M. Tranquada, A. Kapitulnik, and C. Howald, Rev. Mod. Phys. **75**, 1201 (2003).
[18] R.S. Markiewicz, J. Phys. Chem. Solids **58**, 1179 (1997).
[19] J.M. Tranquada, B.J. Sternlieb, J.D. Axe, Y. Nakamura, and S. Uchida, Nature **375**, 561 (1995); J.M. Tranquada, J.D. Axe, N. Ichikawa, A.R. Moodenbaugh, Y. Nakamura, and S. Uchida, Phys. Rev. Lett **78**, 338 (1997).
[20] M. Enoki, M. Fujita, T. Nishizaki, S. Iikubo, D.K. Singh, S. Chang, J.M. Tranquada, and K. Yamada, Phys. Rev. Lett. **110**, 017004, (2013).
[21] K. Yamada, C. H. Lee, K. Kurahashi, J. Wada, S. Wakimoto, S. Ueki, H. Kimura, Y. Endoh, S. Hosoya, G. Shirane, R. J. Birgeneau, M. Greven, M. A. Kastner, and Y. J. Kim, Phys. Rev. B **57**, 6165 (1998).
[22] W.D. Wise, Kamalesh Chatterjee, M.C. Boyer, Takeshi Kondo, T. Takeuchi, H. Ikuta, Zhijun Xu, Jinsheng Wen, G.D. Gu, Yayu Wang, and E.W. Hudson, Nature Physics **5**, 213 (2009).
[23] T. Wu, H. Mayaffre, S. Krämer, M. Horvatić, C. Berthier, W.N. Hardy, Ruixing Liang, D.A. Bonn, and M.-H. Julien, Nature **477**, 191 (2011).
[24] G. Ghiringhelli, M. Le Tacon, M. Minola, S. Blanco-Canosa, C. Mazzoli, N. B. Brookes, G.M. De Luca, A. Frano, D.G. Hawthorn, F. He, T. Loew, M. Moretti Sala, D.C. Peets, M. Salluzzo, E. Schierle, R. Sutarto, G.A. Sawatzky, E. Weschke, B. Keimer, and L. Braicovich, Science **337**, 821 (2012).
[25] A.J. Achkar, R. Sutarto, X. Mao, F. He, A. Frano, S. Blanco-Canosa, M. Le Tacon, G. Ghiringhelli, L. Braicovich, M. Minola, M. Moretti Sala, C. Mazzoli, Ruixing Liang, D.A. Bonn, W.N. Hardy, B. Keimer, G.A. Sawatzky, and D.G. Hawthorn, Phys. Rev. Lett. **109**, 167001 (2012).
[26] J. Chang, E. Blackburn, A.T. Holmes, N.B. Christensen, J. Larsen, J. Mesot, Ruixing Liang, D.A. Bonn, W.N. Hardy, A. Watenphul, M. v. Zimmermann, E.M. Forgan, and S.M. Hayden, Nature Physics **8**, 871 (2012).
[27] D. LeBoeuf, S. Krämer, W.N. Hardy, Ruixing Liang, D.A. Bonn, and C. Proust, Nature Physics **9**,79 (2013),.
[28] E. Blackburn, J. Chang, M. Hucker, A.T. Holmes, N.B. Christensen, Ruixing Liang, D.A. Bonn, W N. Hardy, M. v. Zimmermann, E.M. Forgan, and S.M. Hayden, Phys.

Rev. Lett. **110**, 137004 (2013).
[29] I. Zeljkovic, Z. Xu, J. Wen, G. Gu, R. S. Markiewicz, and J. E. Hoffman, Science 337, 320 (2012).
[30] A.C. Fang, L. Capriotti, D.J. Scalapino, S.A. Kivelson, N. Kaneko, M. Greven, and A. Kapitulnik, Phys. Rev. Lett. **96**, 017007 (2006).
[31] R.S. Markiewicz. Phys. Rev. B. **62**, 1252 (2000).
[32] J.D. Jorgensen, B. Dabrowski, S. Pei, D.G. Hinks, L. Soderholm, B. Morosin, J.E. Schirber, E.L. Venturini, and D.S. Ginley, Phys. Rev. B**38**,11337 (1988); M.F. Hundley, J.D. Thompson, S.-W. Cheong, Z. Fisk, and J.E.Schirber, Phys. Rev. B**41**, 4062 (1990); P.C. Hammel, A.P. Reyes, Z. Fisk,M. Takigawa, J.D. Thompson, R.H. Heffner, S.-W. Cheong, and J.E. Schirber, Phys.Rev. B **42**, 6781 (1990).
[33] There should also be minigaps, but we assume these are washed out by fluctuations and disorder.
[34] C. Kusko, R. S. Markiewicz, M. Lindroos, and A. Bansil, *Phys. Rev. B.* **66**, 140513(R) (2002).
[35] K.M. Shen, T. Yoshida, D.H. Lu, F. Ronning, N.P. Armitage, W.S. Lee, X.J. Zhou, A. Damascelli, D.L. Feng, N.J.C. Ingle, H. Eisaki, Y. Kohsaka, H. Takagi, T. Kakeshita, S. Uchida, P.K. Mang, M. Greven, Y. Onose, Y. Taguchi, Y. Tokura, Seiki Komiya, Yoichi Ando, M. Azuma, M. Takano, A. Fujimori, and Z.-X. Shen, Phys. Rev. B **69**, 054503 (2004).
[36] Z. -H. Pan, P. Richard, Y. -M. Xu, M. Neupane, P. Bishay, A. V. Fedorov, H. -Q. Luo, L. Fang, H. -H. Wen, Z. Wang, and H. Ding, Phys. Rev. B **79**, 092507 (2009).
[37] S. Lupi, D. Nicoletti, O. Limaj, L. Baldassarre, M. Ortolani, S. Ono, Yoichi Ando, and P. Calvani, Phys. Rev. Lett. **102**, 206409 (2009).
[38] I.M. Vishik, M Hashimoto, R.-H. He, W.S. Lee, F. Schmitt, D.H. Lu, R.G. Moore, C. Zhang, W. Meevasana, T. Sasagawa, S. Uchida, K. Fujita, S. Ishida, M. Ishikado, Y. Yoshida, H. Eisaki, Z. Hussain, T.P. Devereaux, and Z.-X. Shen, PNAS **109**, 18332 (2012).
[39] A. L. Efros. J. Phys. C: Solid State Phys. **9** 2021 (1976).
[40] Yingying Peng, Jianqiao Meng, Daixiang Mou, Junfeng He, Lin Zhao, Yue Wu, Guodong Liu, Xiaoli Dong, Shaolong He, Jun Zhang, Xiaoyang Wang, Qinjun Peng, Zhimin Wang, Shenjin Zhang, Feng Yang, Chuangtian Chen, Zuyan Xu, T.K. Lee, X.J. Zhou. Nature Communications **4**, 2459 (2013).
[41] E.L. Nagaev, "Physics of Magnetic Semiconductors" (Moscow, Mir, 1983).
[42] G. Drachuck, E. Razzoli, G. Bazalitski, A. Kanigel, C. Niedermayer, M. Shi, and A. Keren, Nature Communications **5**, doi:10.1038/ncomms4390.
[43] Parameters used are x_0=0.0, x_1=0.09, with $Z = 0.9$ and $Z = 0.7$ respectively. Δ=153meV in (a) and 20meV in (b).
[44] Here, x_0=0.0, x_1=0.09, with $Z = 1$ and $Z = 0.5$ respectively, and Δ=82.4meV with $x_{av} = 0.03$.